https://doi.org/10.2352/EI.2026.38.8.IQSP-252

MTF and aliasing characterization of Photon Router CMOS image sensor

Yuyao Chen, Yahya Mohtashami, Zhiqiang Lin, Dyson (HsinChih) Tai, and Eiichi Funatsu
OMNIVISION Technologies, Inc., Santa Clara, CA, USA

Abstract

Photon router technology is emerging as a novel approach that replaces microlenses to boost CMOS image sensor signal-to-noise ratio. It provides an approach to solve the signal-to-noise ratio drop associated with the trend of pixel size reduction. To comprehensively understand the photon router image sensors overall image quality, it is critical to study the modulated transfer function and aliasing effect. In this study, we show that photon routers exhibit lower sensor MTF compared to the microlenses due to its higher effective fill factor. Our image simulations show that photon routers present less severe aliasing artifacts compared to the microlenses. We show that it is because lower MTF of photon routers leads to lower aliasing components. Furthermore, we present that the reduced resolution in the photon router image can be effectively compensated through tuning sharpening parameter in the image signal processing, enabling comparable sharpness. Our findings highlight the trade-off between achieving high signal-to-noise ratio and high modulated transfer function for photon routers and provide design insights for next-generation high-performance CMOS image sensors.

Introduction

Over the past few decades, the demand for capturing high-resolution images has driven the pixel size shrinkage of CMOS image sensors. However, as the pixel size decreases, the photon number received by each pixel reduces proportionally to the pixel area. This results in a lower signal-to-noise ratio (SNR) at a given illuminance for small pixel image sensors. Recently, multiple Photon Routing (PR) technologies have been proposed to replace the microlens (ML) for achieving higher SNR [1-3]. As shown in Fig. 1 schematics, the PR substitutes microlenses with multi-layered nanopillar arrays. The PR can collect light at the desired wavelengths for a pixel from an area larger than the pixel size, while the ML can only collect from an area equal to the pixel size. Therefore, PR can enhance the SNR by increasing the light collection area at desired wavelength for each pixel.

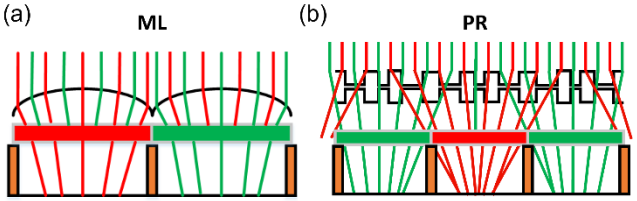

Figure 1. *The side-view schematics of light incident onto red and green pixels for (a) ML and (b) PR sensor.*

Except for SNR, the modulated transfer function (MTF) is also crucial for image quality assessment. In this study, we focus on the MTF and aliasing analysis for ML and PR CMOS image sensors. First, we report the ML and PR sensor MTF results, where PR exhibits lower MTF with respect to ML. To explain the MTF reduction for PR, we develop a general MTF model for Bayer-pattern sensors. We fit the ML and PR MTF curves by tuning the fill factor (ff) and demonstrate that the PR exhibits a lower MTF because it corresponds to a higher ff. Furthermore, we perform image simulations to study the aliasing effect of ML and PR. We show that the PR image presents less aliasing than ML, which is consistent with its lower aliasing components in the imaging system MTF. Finally, by tuning image signal processing (ISP) sharpening parameters, we demonstrate that PR's image resolution can be improved to approach that of the ML. This suggests a practical pathway to compensate PR's resolution loss while leveraging its SNR advantages.

MTF characterization and modeling

We performed the sensor MTF simulations for both the ML and PR at pixel size $p = 2.1\mu m$ using the finite-difference time-domain method. We illuminated the sensor under green light at the wavelength of $\lambda = 540nm$ in the simulation. The obtained sensor MTF results are shown in Fig. 2. The results clearly showed that PR has a lower sensor MTF compared to ML. Specifically, PR showed a 13% MTF drop at the 0.25 cycl/pixel spatial frequency compared to the ML. It indicates that PR images will have lower resolution.

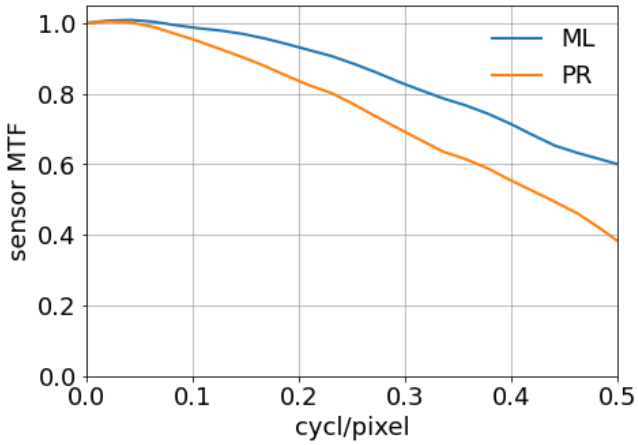

Figure 2. *ML and PR sensor MTFs from full-wave simulations.*

To understand the MTF drop of PR image sensor, it is important to establish a model that accurately characterizes the MTF curves related to sampling patterns. The sampling pattern schematics for ML and PR green channels are shown in Fig. 3 (a) and (b). We can clearly see that the PR collects light for green pixels from a larger area compared to ML, leading to the sensitivity boost.

The general sensor MTF expression in one dimension can be derived as follows:

$$MTF_{sensor} = sinc(d \cdot ff \cdot f) \quad (1)$$

, where the $sinc(x) = sin(\pi x)/(\pi x)$, d is the sensor sampling periodicity, ff is the fill factor, and f is the spatial frequency. The fill factor is defined as the ratio of the pixel's light-sensitive area for the wavelength of interest to the periodic sampling periodicity.

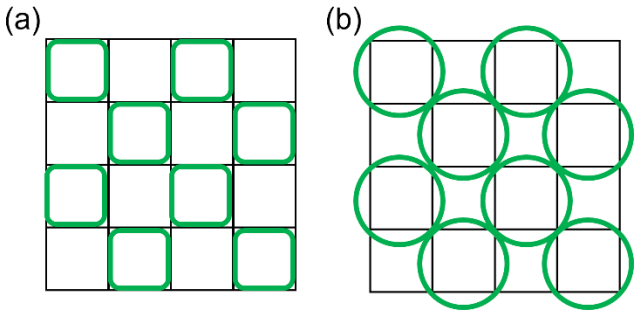

Figure 3. *The light sampling pattern for green channels in the Bayer pattern for (a) ML and (b) PR.*

For the Bayer sampling pattern shown in Fig. 3, $d = 2p$. The ML sensor corresponds to $ff \approx 0.5$ since half of the Bayer pattern is collecting green light along both dimensions. The PR should correspond to $ff > 0.5$ as each green pixel is sampling from a window larger than the pixel area.

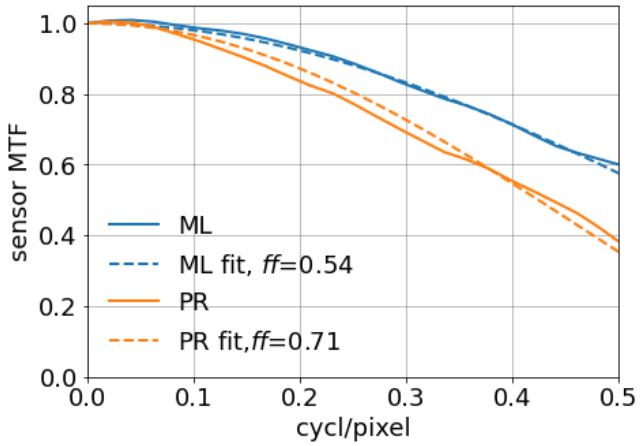

Figure 4. *Fitting results of ML and PR sensor MTF based on Equation 1 by varying the fill factor ff.*

We used Equation 1 to fit the ML and PR MTF curves by varying ff in Equation 1. The fitting results are plotted in Fig. 4, where we obtain good agreement between MTF fit results and the ML and PR MTFs. In particular, the ML and PR MTFs correspond to the ff=0.54 and ff=0.71, respectively. Therefore, a higher fill factor of PR boosts SNR but leads to a lower sensor MTF. The results align with the schematics shown in Fig. 3.

Aliasing effect characterization

Besides SNR and MTF, the aliasing effect also plays a critical role in image quality. It can result in visually disturbing color Moiré artifacts. We performed image simulations using the Siemens star target in camera simulator we developed. Such an object can visually demonstrate the aliasing differences between ML and PR. We applied Gamma correction with $\gamma = 2.2$ and used the bilinear demosaic method. The simulated ML and PR images are shown in Fig. 5 (a) and (b), respectively.

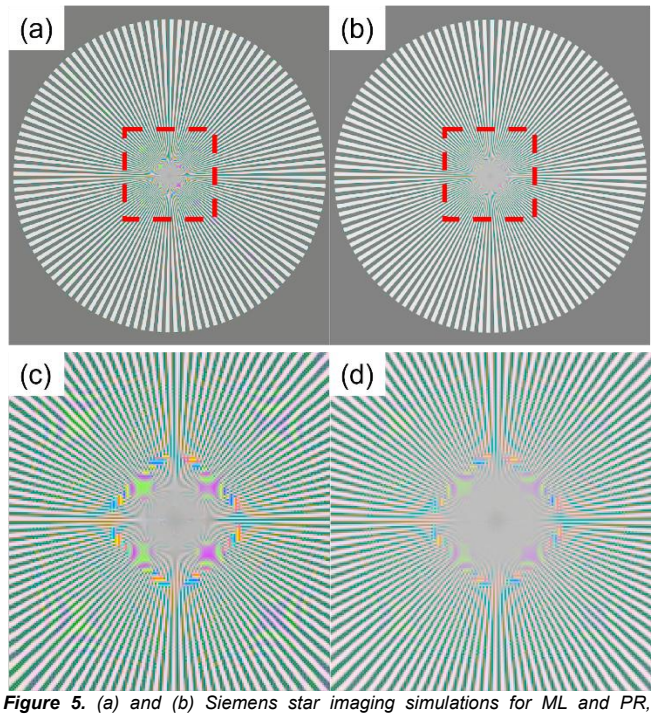

Figure 5. *(a) and (b) Siemens star imaging simulations for ML and PR, respectively. (c) and (d) Zoom-in views of the center regions as indicated by the red dashed squares in (a) and (b).*

To better visualize the aliasing effect, we show the zoom-in views of the Siemens star center region in Fig 5. (c) and (d) for ML and PR, respectively. We can clearly observe that the simulated ML image shows stronger color Moiré in Fig 5. (c). To understand the aliasing effects difference, we characterized the aliasing components for the ML and PR image system, which consists of a module lens and ML or PR sensors. Thus, the system MTF is the product of the module lens and the sensor MTF. We assumed here that a homogeneous circular aperture module lens is used for ideal incoherent imaging. The module lens MTF then depends only on the F-number and operating wavelength [4]. We used F-number 1.6 and operating wavelength 540nm for the module lens. The corresponding system MTFs of ML and PR are shown in Fig. 6.

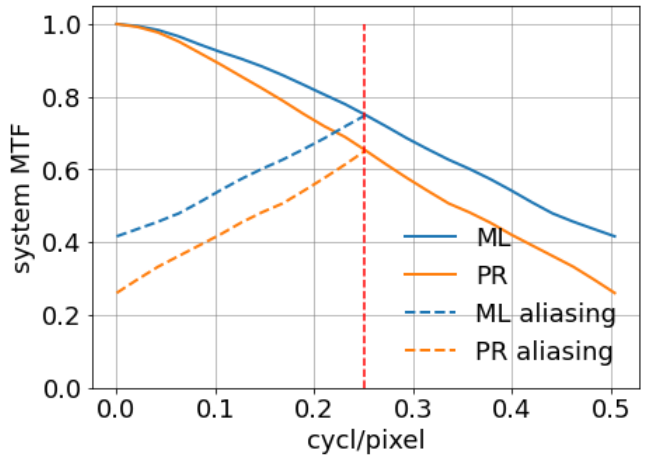

Figure 6. *ML and PR system MTF and corresponding aliasing components*

Furthermore, according to the Nyquist sampling theory, the high-frequency part of the MTF above the Nyquist frequency cannot be correctly captured. It is folded back to the lower frequency side and becomes the aliasing component. For an image sensor with Bayer pattern, the Nyquist frequency is half of the sampling frequency, $f_{Nyquist} = 1/(2d) = 0.25$ cycl/pixel. We highlighted the Nyquist frequency position in Fig. 6 using the red dashed line. The corresponding aliasing components are also shown for the green channel. We can see that the aliasing component of PR is lower than that of ML. This explains our visual observations in Fig. 5. Therefore, despite PR having a lower MTF, it exhibits less color aliasing than ML under the same module lens.

Resolution loss and sharpening tuning

We presented in the previous part that the PR's sensor MTF is lower than ML. To appreciate the resolution difference, image simulations are performed using the ISO chart as the target. Specifically, we show the zoom-in views of the wedge segment of the ISO chart for ML and PR in Fig. 7 (a) and (b), respectively. We used the same image signal processing (ISP) parameter for ML and PR images. The wedges around the digit '14' in ML image show higher contrast than the PR image. It agrees with the result that ML has a higher sensor MTF.

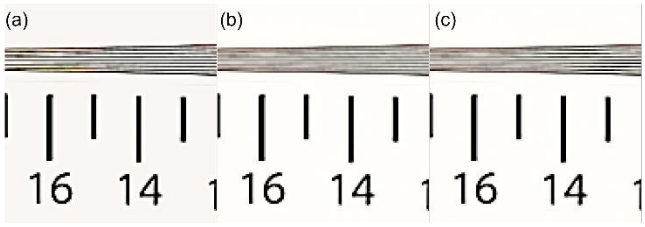

Figure 7. *(a) and (b) Zoom-in views of the ISO chart wedge segment for ML and PR, respectively, using the same ISP parameters. (c) PR with enhanced sharpening in ISP.*

Additionally, we increased the sharpening parameter in ISP for the PR image. The image of PR after sharpening enhancement is shown in Fig. 7 (c). The wedge contrast is comparable to ML after ISP tuning. Therefore, we can compensate for the PR resolution loss by tuning the ISP parameter. Note that the wedges in the PR image around the digit '16' still look blurry after tuning. It is in the aliasing region where the number of wedges cannot be correctly captured. The resolution comparison in the aliasing region is not reliable since the image does not represent the underlying signal correctly.

Conclusion

In conclusion, we characterized the sensor MTF for Bayer-pattern CMOS image sensors based on ML and PR technologies. We presented an MTF model that accurately characterizes the obtained MTF curves. We showed that the PR MTF is lower than the ML because it has a larger fill factor. Furthermore, we quantified the aliasing effects inherent to ML and PR on their imaging system MTFs, revealing their critical impact on image quality. We performed image simulations using the Siemens star target to visualize these aliasing artifacts. Finally, we demonstrated that tuning the sharpening parameters in ISP can effectively mitigate the resolution loss observed in PR sensors. Our study provided a more comprehensive picture of image quality when evaluating the MTF of PR and ML. It paves the way for next-generation high-SNR, high-quality PR-based CMOS image sensors.

References

[1] Peter B. Catrysse, et al., "Subwavelength Bayer RGB color routers with perfect optical efficiency." Nanophotonics 11(10), 2381–2387 (2022).

[2] Chulsoo Choi, et al., "Optical Design of Dispersive Metasurface Nano-Prism Structure for High Sensitivity CMOS Image Sensor." Proceedings of the 2023 International Electron Devices Meeting (IEDM) (Dec 2023)

[3] Chun-Yuan Wang, et al., "CMOS image sensor with nano light pillars for optical performance enhancement," Proceedings of the 2023 International Electron Devices Meeting (IEDM) (Dec 2023)

[4] J. W. Goodman, "Introduction to Fourier Optics", Greenwood Village, CO, Roberts & Co. (2005).

Author Biography

Yuyao Chen received his PhD in Electrical Engineering from Boston University (2022). He works now as a Staff Image Sensor Technology Engineer at OMNIVISION Technologies, Inc., CA. His work focused on optical structure simulation and inverse design.

JOIN US AT THE NEXT EI!

electronic IMAGING

Imaging across applications . . . Where industry and academia meet!

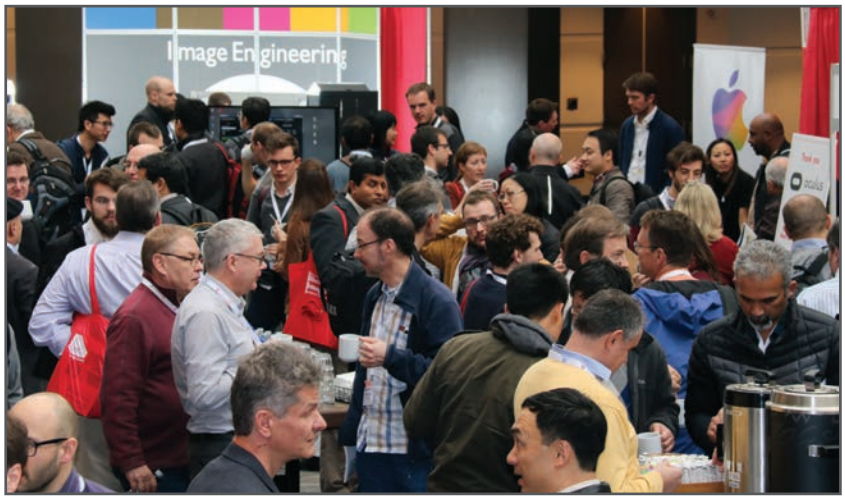

• SHORT COURSES • EXHIBITS • DEMONSTRATION SESSION • PLENARY TALKS •
• INTERACTIVE PAPER SESSION • SPECIAL EVENTS • TECHNICAL SESSIONS •

www.electronicimaging.org

ADVANCING IMAGING SCIENCE 75 1947 IS&T 2022 imaging.org